SIAM. J. APPL. MATH.
Vol. 52, No. 2, pp. 459-484, April 1992

011

LOCAL TOMOGRAPHY*

ADEL FARIDANI†, ERIK L. RITMAN‡, AND KENNAN T. SMITH†

Abstract. Tomography produces the reconstruction of a function f from a large number of line integrals of f. Conventional tomography is a global procedure in that the standard convolution formulas for reconstruction at a single point require the integrals over all lines within some plane containing the point. Local tomography, as introduced initially, produced the reconstruction of the related function Λf, where Λ is the square root of $-\Delta$, the positive Laplace operator. The reconstruction of Λf is local in that reconstruction at a point requires integrals only over lines passing infinitesimally close to the point, and Λf has the same smooth regions and boundaries as f. However, Λf is cupped in regions where f is constant. $\Lambda^{-1} f$, also amenable to local reconstruction, is smooth everywhere and contains a counter-cup. This article provides a detailed study of the actions of Λ and Λ^{-1}, and shows several examples of what can be achieved with a linear combination. It includes the results of x-ray experiments in which the line integrals are obtained from attenuation measurements on two-dimensional image intensifiers and fluorescent screens, instead of the usual linear detector arrays.

Key words. 2D-CT, 3D-CT, tomography, local, x-rays, image enhancement, image intensifiers

AMS(MOS) subject classifications. 45L10, 65R10

Introduction. Tomography produces the reconstruction of a generalized density function f from a large number of line integrals of f. In x-ray tomography, the density function is the x-ray attenuation coefficient, and the line integrals are obtained by measuring the attenuation of photons transmitted through the object. Photons are emitted from several hundred x-ray sources, and the attenuation is measured along several hundred lines through each source.

Formulas for reconstructing f from such data involve the convolution of the data from each source with a fixed kernel k that is rarely 0. The standard formulas for reconstruction at a single point require attenuation measurements along all lines within some plane containing the point.

Local tomography produces the reconstruction of the related function $\Lambda f + \mu \Lambda^{-1} f$, where Λ is the square root of $-\Delta$, the positive Laplace operator. The reconstruction of $\Lambda f + \mu \Lambda^{-1} f$ is local: for reconstruction at a point, attenuation measurements are needed only along lines very close to that point. Since Λ is an invertible elliptic operator, f and Λf have precisely the same singularities, e.g., boundaries between regions of constant density, and these boundaries are sharper in Λf. However, Λf is cupped, not constant, within regions of constant density. The cup is largely neutralized by the addition of $\mu \Lambda^{-1} f$. Local tomography was introduced in [9] and [12] without the cup correction.

In practice, the typical density function is constant (or almost constant) in each of a finite number of sets, i.e., is a linear combination of characteristic (indicator) functions of sets. Insight into the nature of local tomography is obtained by studying its application to the characteristic function χ_X of a set $X \subset R^n$.

It turns out that $\Lambda \chi_X$ dies rapidly away from X, and, near X, is roughly proportional to $\pm d(x, \partial X)^{-1}$ (+ inside X, − outside), where $d(x, \partial X)$ denotes the distance from x

* Received by the editors June 4, 1990, accepted for publication November 10, 1990. This research has been supported by the Alexander von Humboldt Foundation, National Science Foundation grant DMS87-2716, and National Institutes of Health grant HL04664.

† Mathematics Department, Oregon State University, Corvallis, Oregon 97331.

‡ Biodynamics Research Unit, Mayo Clinic, Rochester, Minnesota 55901.

to the boundary of X. On the other hand, $\Lambda^{-1}\chi_X$ behaves like $c+d(x,\partial X)$ inside, and like $(c+d(x,\partial X))^{1-n}$ outside. (c is a constant depending mainly on the curvature of the boundary of X.) Somewhat surprisingly, the cup in $d(x,\partial X)^{-1}$ is neutralized by the counter-cup in $c+d(x,\partial X)$. While $\Lambda f+\mu\Lambda^{-1}f$ is not an approximation to f, it provides a remarkably similar qualitative representation. Several examples are shown in § 2.

It also turns out that, inside X, the minimum of $\Lambda\chi_X$ is roughly proportional to $\delta(X)^{-1}$, where $\delta(X)$ is the diameter of X.

In practice, the jump in $\Lambda\chi_X$ at the boundary of X is, of course, smoothed, but it is still large, providing very sharp and visible boundaries between regions of different density. The dependence of $\Lambda\chi_X$ on the diameter of X increases the apparent density contrast of small sets, thereby making small sets with low density contrast more visible. Neither characteristic of Λ is changed by adding a multiple of Λ^{-1}.

During the past year, local tomography has become the standard procedure at the Biodynamics Research Unit of the Mayo Clinic for defining the anatomic outline of the lungs and for the study of the coronary arterial tree. With regular tomography, the lung edge is sufficiently blurred that no consistent edge is detected, while consistent edges are detected with the sharp boundaries of local tomography. With a noninvasive minimal intravenous dye injection, the coronary tree presents small sets of low density contrast, the study of which is facilitated by the enhancement of local tomography.

The computational advantage of local tomography stems from the fact that the local convolution kernel K is nonzero at very few points, usually 3–8 (depending on the noise), as opposed to several hundred in standard kernels. This reduces the number of multiplications per convolution value to 3–8. When only a part of the object must be reconstructed, it reduces proportionately the amount of data collected and processed, and the x-ray dose.

Local tomography has other features that become particularly useful if the attenuation data are collected two-dimensionally. For example, in current three-dimensional heart studies, two-dimensional attenuation data are measured on a 30 cm. × 30 cm. fluorescent screen spanning the full chest, then demagnified optically to a $\sim$1 cm^2 CCD chip. Reducing the span to the heart itself dramatically reduces the required dynamic range of the detection system, the geometric distortions, and the optical inefficiencies entailed in demagnification. An example of the improvement effected by coning the x-ray beam to the heart is described in [11].

Another feature of local tomography with two-dimensional attenuation measurements is that other, and more efficient, measurement devices than the fluorescent-screen–demagnifying-lens combination can be used when the part reconstructed is not too large. Specifically, it is expected that commercially available fluoroscopic systems will provide useful images. An example is shown in § 2.

Sections 1 and 2 describe notation, definitions, and basic results of the paper in terms accessible to nonmathematical tomographers. Section 2 shows examples, as well. Sections 3–8 contain the proofs of the results described in § 2, along with some refinements. Section 9 describes the algorithm used for most of the examples. The Appendix contains the basic mathematical formulas of tomography. To tomographers who do not want quantitative information, this introduction and the examples in § 2 should indicate the possibilities in local tomography. To those who do want quantitative results but not proofs, the theorems in § 2 should provide them.

1. Standard notation and definitions. R^n consists of n-tuples of real numbers, usually designated by single letters, $x=(x_1,\cdots,x_n)$, $y=(y_n,\cdots,y_n)$, etc. The inner

product and absolute value are defined by

$$\langle x, y\rangle = \sum_1^n x_j y_j \quad \text{and} \quad |x| = \langle x, x\rangle^{1/2}. \tag{1.1}$$

The unit sphere S^{n-1} consists of the points of absolute value 1. A point on S^{n-1} usually is designated by θ.

If X is a subset of R^n, X', X°, $\bar{X}$, and ∂X denote the complement, interior, closure, and boundary. χ_X is the characteristic function of X, equal to 1 on X, and 0 on X'. The diameter of X, $\delta(X)$, is the upper bound of the distances $|x-y|$ between points x and y of X. If Y is another subset, the distance from X to Y, $d(X, Y)$, is the lower bound of $|x-y|$ for $x \in X$ and $y \in Y$.

$|X|$ denotes the n-dimensional Lebesgue measure of X. However, when it is clear that X should be treated as a set of dimension $k < n$, $|X|$ is the k-dimensional area measure. Thus $|S^{n-1}|$ and $|S^{n-2}|$ are the $(n-1)$- and $(n-2)$-dimensional area measures of the $(n-1)$- and $(n-2)$-dimensional spheres. Explicitly,

$$|S^{n-1}| = 2\pi^{n/2}/\Gamma(n/2). \tag{1.2}$$

($|S^{n-1}|$ and $|S^{n-2}|$ appear as constants in several theorems.) In integrals over R^n, the measure is denoted by dx; in integrals over S^{n-1}, the measure is denoted by $d\theta$. For $n = 2$, the latter is arc length on the unit circle.

When functions or distributions f and g lie in dual spaces, the scalar product is denoted by $\langle f, g\rangle$. If both are functions, the scalar product is usually given by an integral:

$$\langle f, g\rangle = \int f(x) g(x)\, dx. \tag{1.3}$$

The Fourier transform is defined by

$$\hat{f}(\xi) = (2\pi)^{-n/2} \int e^{-i\langle x,\xi\rangle} f(x)\, dx \tag{1.4}$$

for integrable functions f, and is extended to larger classes of functions or distributions by continuity or duality.

For $s \geqq 0$, H^s denotes the Sobolev space of functions $f \in L^2$ with

$$\|f\|_s^2 = \int (1+|\xi|^2)^s |\hat{f}(\xi)|^2\, d\xi < \infty, \tag{1.5}$$

and H^{-s} is the dual space. H^{-s} is identified with the space of tempered distributions g for which $\hat{g}$ is a function satisfying

$$\|g\|_{-s}^2 = \int (1+|\xi|^2)^{-s} |\hat{g}(\xi)|^2\, d\xi < \infty. \tag{1.6}$$

The scalar product between $f \in H^s$ and $g \in H^{-s}$ is given by (1.3) on the Fourier transform side.

The operator Λ, which became well known through the pioneering work of Calderón in partial differential equations, and which now pervades tomography, is defined in terms of Fourier transforms by

$$(\Lambda f)\hat{}\,(\xi) = |\xi| \hat{f}(\xi) \tag{1.7}$$

for functions in the Sobolev space H^1. Λf is defined for more general functions and distributions by duality as

$$\langle \Lambda f, \varphi\rangle = \langle f, \Lambda\varphi\rangle \quad \text{for } \varphi \in C_0^\infty, \tag{1.8}$$

the space of infinitely differentiable functions with compact support. The existence of Λf as a distribution requires a condition on f at ∞. A convenient condition that admits all characteristic functions of measurable sets is

$$f(1+|x|)^{-1-n} \in L^1. \tag{1.9}$$

This is discussed in § 3.

For $n \geqq 2$, Λ^{-1}, the inverse of Λ, is the convolution operator $R_1 * f$,

$$R_1 * f(x) = \int R_1(x-y) f(y)\, dy, \tag{1.10}$$

where R_1 is the inverse Fourier transform of $(2\pi)^{-n/2}|\xi|^{-1}$, i.e., is the Riesz kernel

$$R_1(x) = (1/(\pi|S^{n-2}|))|x|^{1-n}.$$

Wherever R_1 appears in the sequel, it is assumed, sometimes tacitly, that $n \geqq 2$.

2. Results and examples. The typical objects studied in tomography are made up of regions of nearly constant density, so the density function f is essentially a linear combination of characteristic functions of sets. Insight into the nature of local tomography can be obtained by studying $\Lambda\chi_X$, where X is a measurable set in R^n, $n \geqq 2$.

THEOREM 2.1. *Let X and Y be measurable sets.*

(a) *If $f_r(x) = f(x/r)$, then $\Lambda f_r(x) = r^{-1}\Lambda f(x/r)$.*

(b) *$\Lambda\chi_X$ is an analytic function on $(\partial X)' = R^n - \partial X$.*

(c) *$\Lambda\chi_X(x) > 0$ on X°, and < 0 on X'°; $\Lambda\chi_{X'} = -\Lambda\chi_X$.*

(d) *If $X \subset Y$, then*

$$|\Lambda\chi_X(x)| \geqq |\Lambda\chi_Y(x)| \text{ on } X^\circ,\ |\Lambda\chi_X(x)| \leqq |\Lambda\chi_Y(x)| \text{ on } Y'^\circ.$$

(e) *If x is not on ∂X, then*

$$\pi d(x, \partial X)|\Lambda\chi_X(x)| \leqq (n-1)|S^{n-1}|/|S^{n-2}|.$$

(f) *If X has finite measure, then on X'°*

$$\pi d(x, \partial X)|\Lambda\chi_X(x)| \leqq ((n-1)/|S^{n-2}|)|X| d(x, \partial X)^{-n}.$$

THEOREM 2.2. *$\Lambda\chi_X$ is subharmonic (Laplacian $\geqq 0$) on X°, and superharmonic on X'°. This implies that*

(a) *$\Lambda\chi_X$ cannot have a local maximum in X°, nor a local minimum in X'°.*

(b) *For $a \in X^\circ$, the average of $\Lambda\chi_X$ over the sphere with center a and radius r is an increasing function of r on $r < d(a, \partial X)$.*

(c) *Fix a (anywhere). If X is contained in the ball with center a and radius r_0, r^{n-2} times the average of $-\Lambda\chi_X$ over the sphere with center a and radius r is a decreasing function of r on $r > r_0$.*

When the boundary of X has some smoothness, the inequality in part (e) of Theorem 2.1 can be sharpened and reversed, the sharpness depending on the smoothness.

THEOREM 2.3. *If X is a half-space, $\pi d(x, \partial X)|\Lambda\chi_X(x)| = 1$. If X is convex, $\pi d(x, \partial X)|\Lambda\chi_X(x)| \geqq 1$ on X°, and $\leqq 1$ on X'°.*

A less sharp inequality holds when X' contains not an entire half-space tangent to the boundary, but only part of an open cone with vertex on the boundary.

DEFINITION 2.4. $C(\theta, \alpha, \delta)$, the open cone with vertex 0, axis θ, opening angle 2α, and radius δ is defined by

$$C(\theta, \alpha, \delta) = \{x: \langle x, \theta\rangle > |x| \cos(\alpha), |x| < \delta\}.$$

THEOREM 2.5. *Let $x \in X^\circ$, and let $\bar{x}$ be the closest point in ∂X to x. If $\bar{x} + C(\theta, \alpha, \delta) \subset X'$, then $\pi d(x, \partial X)\Lambda\chi_X(x) \geqq c(\delta/(\delta + d(x, \partial X)))^n$, where c depends only on α and n. In particular, if there are constants α and δ so that for each $\bar{x} \in \partial X$ there exist θ and θ' with $\bar{x} + C(\theta, \alpha, \delta) \subset X$ and $\bar{x} + C(\theta', \alpha, \delta) \subset X'$, then there is a constant c depending only on α and n so that, for x not on ∂X,*

$$c(\delta/(\delta + d(x, \partial X)))^n \leqq \pi|\Lambda\chi_X(x)|\, d(x, \partial X) \leqq (n-1)|S^{n-1}|/|S^{n-2}|.$$

When X is bounded and convex and X° is not empty, these latter conditions are satisfied.

The cone condition in Theorem 2.5 is a weak version of the cone condition encountered frequently in partial differential equations, which requires a locally fixed cone axis. It permits any polyhedron X whose boundary is an $n-1$ manifold, which the usual cone condition does not permit. The essential is a "nonthinness" of X' at boundary points. The best conditions have not been investigated, since the weak cone condition is easy to visualize and to use, and it appears to be satisfactory for practice.

When the boundary of X is smooth, $\pi d(x, \partial X)|\Lambda\chi_X(x)|$ is not just bounded above and below as $x \to \partial X$; it approaches 1, and does so rapidly enough that $|\Lambda\chi_X(x) - (1/(\pi d(x, \partial X))|$ is locally integrable. The smoothness required, which is described in the next definition, is essentially that ∂X is a C^1 surface with normals satisfying a Lipschitz condition. In particular, it holds when ∂X is a C^2 surface. As shown in the theorems of § 7, the result holds locally when ∂X satisfies the local smoothness condition.

DEFINITION 2.6. X has curvature $\leqq 1/r$ (or radius of curvature $\geqq r$) along its boundary if for each point $\bar{x} \in \partial X$ there are open balls $B \subset X$ and $C \subset X'$ of radius r with $\bar{x} \in \bar{B} \cap \bar{C}$.

THEOREM 2.7. *There is a continuous function $\tilde{E}_1$ of one variable satisfying $|1 - \tilde{E}_1(|x|)| \leqq C|1-|x||^{1/2}$ such that if X has curvature $\leqq 1/r$ along its boundary, then, for $d(x, \partial X) < r$,*

$$\tilde{E}_1(1 + (d(x, \partial X)/r)) \leqq \pi d(x, \partial X)|\Lambda\chi_X(x)| \leqq \tilde{E}_1(1 - (d(x, \partial X)/r)),$$

$$\big||\Lambda\chi(x)| - (1/(\pi d(x, \partial X))\big| \leqq \mathrm{C} r^{-1/2}\, d(x, \partial X)^{-1/2}.$$

The above theorems show that $\Lambda\chi_X$ dies rapidly away from X; near X, behaves like $d(x, \partial X)^{-1}$; and inside X, has a minimum roughly proportional to $\delta(X)^{-1}$. The following show that $\Lambda^{-1}\chi_X$ behaves like $c + d(x, \partial X)$ inside X, and like $(c + d(x, \partial X))^{1-n}$ outside. It is shown in the Appendix that Λ^{-1} is a convolution operator with kernel R_1, the Riesz kernel of order 1. The definitions and basic properties are explained in the next section. X and Y denote bounded measurable sets. The main results are as follows.

THEOREM 2.8.

(a) *If $f_r(x) = f(x/r)$, then $R_1 * f_r(x) = rR_1 * f(x/r)$.*

(b) *$R_1 * \chi_X$ is continuous on R^n, analytic on $R^n - \partial X$, and subharmonic on X'°.*

(c) *If $X \subset Y$, then $R_1 * \chi_X(x) \leqq R_1 * \chi_Y(x)$ for all x.*

(d) $R_1 * \chi_X(x) \leqq \delta(X)|S^{n-1}|/(\pi|S^{n-2}|)$.

(e) *For $x \in X'$, $R_1 * \chi_X(x) \leqq (|X|/(\pi|S^{n-2}|))d(x, \partial X)^{1-n}$.*

Reverse inequalities come from rather explicit information about balls. According to (a), it is sufficient to treat the unit ball with characteristic function χ.

THEOREM 2.9. *$R_1 * \chi$ is a positive decreasing function of $|x|$. It is a concave function of $|x|$ on $|x| < 1$, and a convex function of $|x|$ on $|x| > 1$.*

THEOREM 2.10. *Let $x \in R^n - \partial X$, let $\bar{x}$ be a point on ∂X at minimum distance from x, and let r be the radius of the largest ball B contained in X, with center on the line*

joining x and $\bar{x}$ and with $\bar{x} \in \bar{B}$. If $C = (n-1)|S^{n-1}|/|S^{n-2}|$, then

$$(n-1)\pi R_1 * \chi_X(x) \geqq (C-2)d(x, \partial X) + 2r \quad \text{for } x \in X^\circ,$$

$$(n-1)\pi R_1 * \chi_X(x) \geqq Cn^{-1}r(1+(d(x, \partial X)/r))^{1-n} \quad \text{for } x \in X'^\circ.$$

The examples below (resolution phantom, head, abdomen, dog chest, and three-dimensional heart) provide comparisons of standard and local tomography in diverse problems, and also comparisons of local tomography with and without the cup correction.

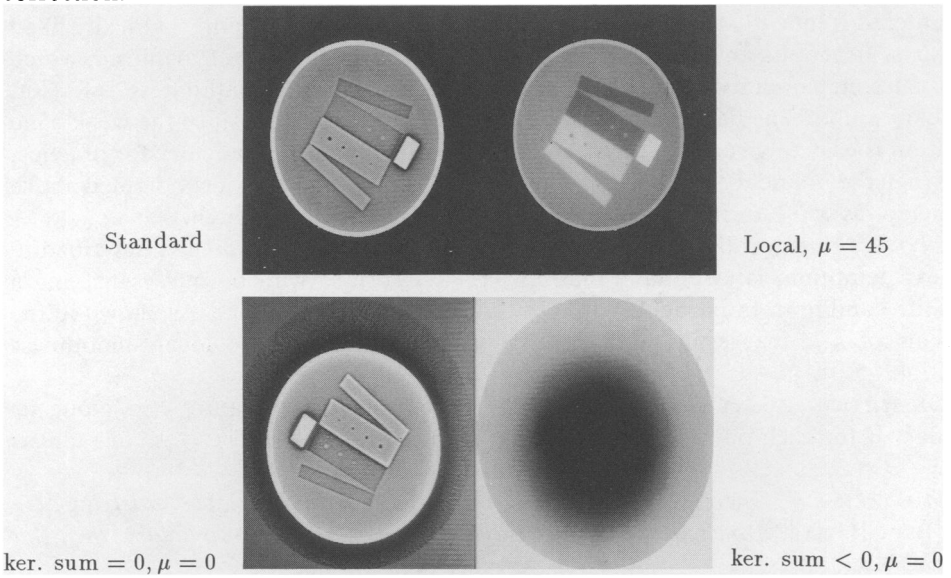

FIG. 1. *Resolution Phantom. The phantom has a diameter of about 25 cm. The densities (x-ray attenuation coefficients) are: exterior: 0, rim: .218, main interior: .195, dense block at left: .372, two upper blocks: .221, two lower blocks: .184, eight small holes in the two central blocks: .195. On the high resolution television monitor, all eight holes are clearly visible.*

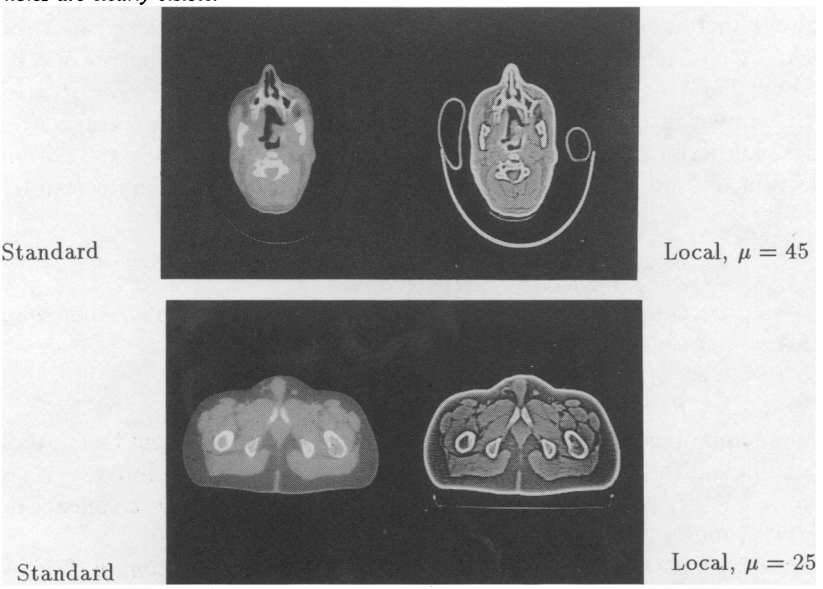

FIG 2. *Typical medical examples. (a) head; (b) abdomen.*

The x-ray data for the phantom, head, and abdomen come from an older-generation Siemens hospital scanner with 720 x-ray sources and 512 detectors. The reconstructions are displayed on 320×320 matrices. (These data were used in [2], where cup corrections were not made, and the algorithms were different.)

The dog chest reconstructions come from the DSR, the fast three-dimensional reconstructor in the Biodynamics Research Unit at the Mayo Clinic, with approximately 3000 x-ray sources and 256 readings per line on the fluorescent screen used for two-dimensional x-ray detection.

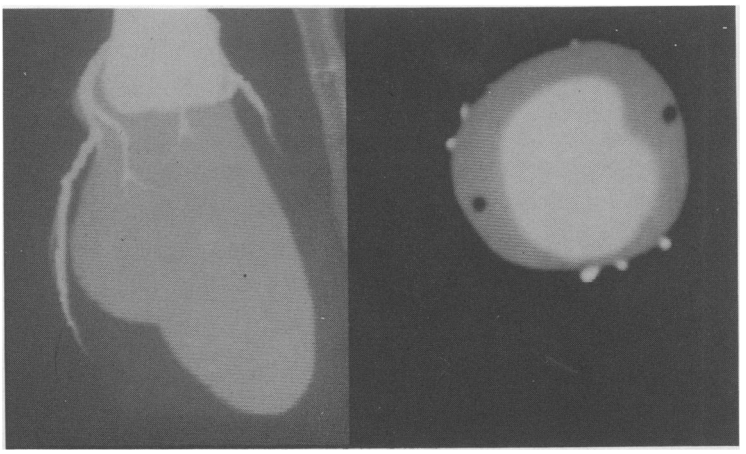

FIG. 3(a). *Standard (Picker 1200 scanner). Apart from the noise, the standard reconstruction and the local cup corrected reconstruction are similar. In both cases the generic cross section is superior to that cross section in the uncorrected reconstruction. However, despite the noise, the arteries are clearer in the uncorrected reconstruction than in either of the others in the three-dimensional projection.Three-dimensional heart, two-dimensional image intensifier detection. The object scanned was a realistic chest phantom, described in detail in* [11]. *The objective was visualization of the coronary arteries. The arteries and chambers contain contrast dye consistent with a minimal intravenous dye injection of about 40 mg iodine per ml blood. In the local reconstruction the attenuation was measured on a two-dimensional 9" bottle image intensifier. The phantom was rotated by hand, so as to provide 314 x-ray sources and 256 readings per source across each horizontal line of the image intensifier. The standard reconstruction was done on a Picker 1200 scanner with 1200 sources and 1024 readings per source across each horizontal line. (With very accurate positioning and about fifteen times the data, the standard reconstruction is much less noisy, but with separate scans of each cross section and a total scan time of several minutes, the standard reconstruction is impractical for beating hearts.) The photos (Figs. 3(a)-(3c)) show two kinds of display: a normal cross section and a three-dimensional projection. The cross section again shows the value of the cup correction, while the projection shows the value of doing without it in some special cases. The projection is made from 120 cross sections assembled in a three-dimensional array. The value of a pixel in the projection plane is the value of the largest voxel along the line through the pixel and perpendicular to the projection plane. After the intravenous dye injection, the coronary arteries and chambers provide the largest voxels. With standard tomography, or with cup-corrected local tomography, the arteries and chambers can be separated in the projection only by manually erasing the chambers in each cross section prior to projection. In local tomography without the cup correction, the cup effect largely removes the chambers. Combined with the enhancement of the contrast of sets with small diameter, this produces arteries brighter than the chambers, therefore arteries visible in the projection. (The projections are useful in localizing and evaluating stenoses, which can then be studied more closely in cross sections if necessary.) In the local reconstructions, the x-ray data are the same for the cup-corrected and uncorrected reconstructions, and the photos show identical views. In the standard reconstruction, the data come from a different scanning device. The cross section and orientations are as close as possible to those in the local reconstructions, but not identical. In these reconstructions, the constants in the formulas were ignored, so the value of μ, which was determined empirically, is not known. As in the other cases, it is a refinement of $\mu = 40$.*

The standard heart reconstructions come from a Picker 1200 scanner with 1200 sources and 1024 detectors. The data for the local reconstructions come from an experimental procedure with a 9″ two-dimensional bottle image intensifier for x-ray detection. There were 314 sources, and each line of the image intensifier was sampled at 256 points. The standard and local reconstructions were done on 150×150 matrices, which were doubled for the display by repeating each row and column.

The standard reconstructions were made with a standard fan-beam algorithm. The local reconstructions were made with the local fan-beam formulas in § 9. The parallel beam kernel occurring in these formulas is the one in formula (A.18) with $m = 11.4174$, a value that leads to a very small kernel sum when the kernel minimum is at detector 1, 2, or 3. For the abdomen and dog chest the kernel minimum was put at detector 2; for the heart, which was quite noisy, it was put at detector 3; for the others (less noisy), it was put at detector 1. Placement of the kernel minimum is discussed in [2]. The reason for a very small kernel sum is discussed in § 9. One of the examples below,

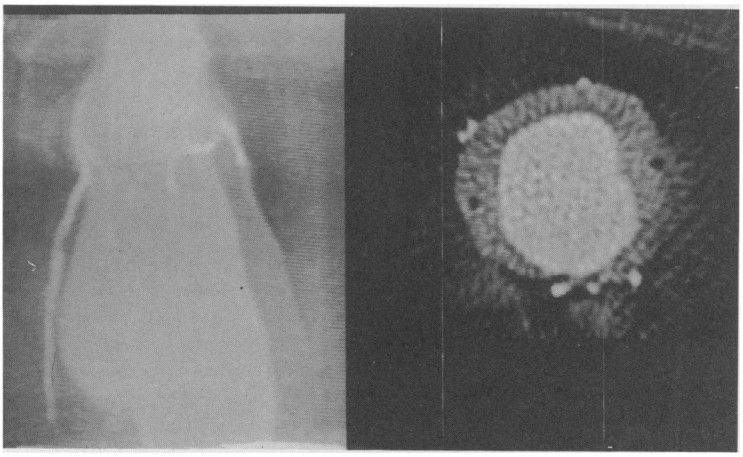

FIG. 3(b). *Local (image intensifier, cup corrected).*

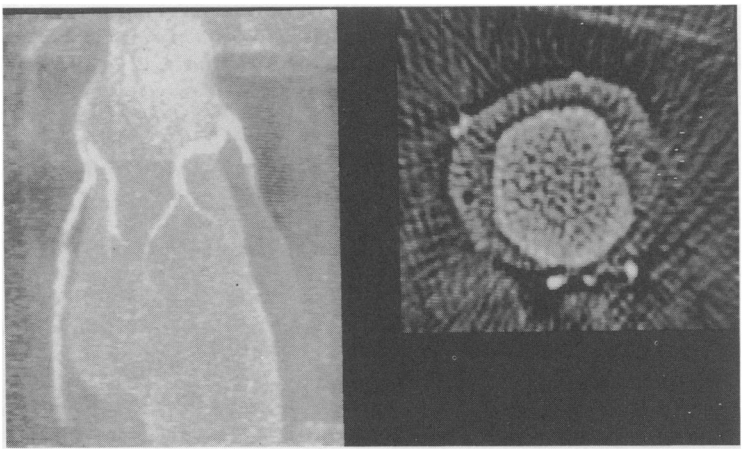

FIG. 3(c). *Local (image intensifier, cup uncorrected).*

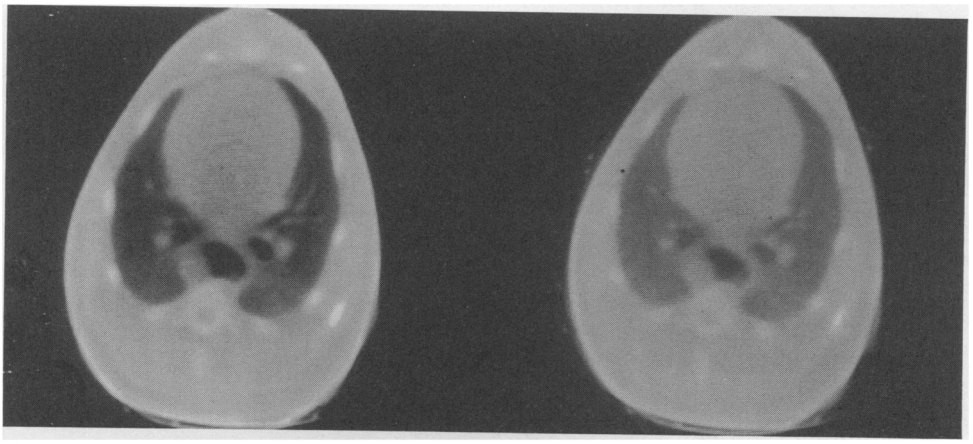

FIG. 4(a) *Standard (fluorescent screen). Lung volume, two-dimensional fluorescent screen detection. Three-dimensional local tomography is being used* [15] *to compute lung volume and changes in lung volume. The scanner, the Mayo Clinic DSR, uses x-ray sources on a circle and two-dimensional fluorescent detection screens to acquire three-dimensional data in about* 0.1 *seconds. Usually, several gated scans are combined to increase the number of x-ray sources and reduce the noise. The pictures (Figs.* 4(*a*) *and* 4(*b*)) *show standard and local reconstructions of one cross section (out of the* 120 *used for the three-dimensional reconstruction) of the chest of a living dog. The gated scans provided the equivalent of* 3300 *x-ray sources, so noise was not a problem, as it was in the previous example with only* 314. *In the local reconstructions, lung boundaries are sharp enough to yield volume calculations consistent with other measurements. The picture show two gray level windowings of the same standard reconstruction, and two local reconstructions, one with a cup correction, the other without. The white dots exterior to the skin are electrodes. The reason for showing two windowings of the standard reconstruction is to show that the electrodes and the exterior circle, which are real, and the familiar exterior boundary artifacts, which are not, are present in the standard reconstruction, too. Their presence, which is clear in the right-hand windowing on the television monitor, but not in the left-hand windowing, is so faint in the photos that it will probably disappear in the reproductions. As in the previous example, the local reconstruction without the cup correction is more useful in the problem at hand (determining sharp lung boundaries), while the reconstruction with the cup correction is more accurate overall.*

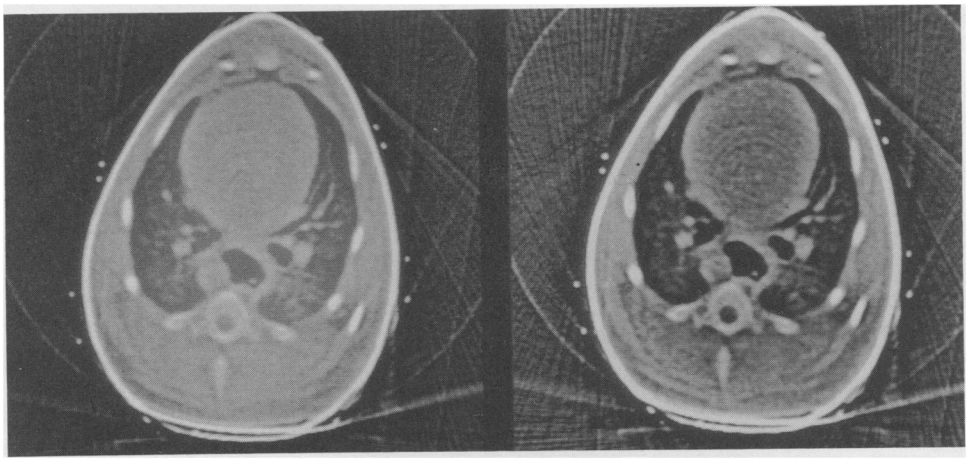

Left: $\mu > 0$. Right: $\mu = 0$

FIG 4(b). *Local (fluorescent screen).*

produced by using $m=6$, shows the effect of a negative kernel sum $\sim 10^{-2}$ times the kernel maximum. In all other examples, $m=11.4174$, and the kernel sum is $\sim 10^{-6}$ times the maximum.

At present there is no theoretical basis for determining the cup correction parameter μ. In the examples studied, a value around 40 gives good pictures, and refinements are easy to achieve empirically. The current results suggest that the primary factor affecting μ is the size of the full object.

In the examples below (Figs. 1 and 2), each reconstruction, standard and local, is windowed separately for an optimal picture.

3. Some facts about Λ and Λ^{-1}. In terms of Fourier transforms, the operator Λ is defined by

$$(\Lambda f)\hat{}(\xi) = |\xi|\hat{f}(\xi) \tag{3.1}$$

for functions $f \in L^2$ with first partial derivatives in L^2, i.e., for functions f in the Sobolev space H^1. Λf is defined for more general functions and distributions by duality:

$$\langle \Lambda f, \varphi\rangle = \langle f, \Lambda\varphi\rangle \quad \text{for } \varphi \in C_0^\infty. \tag{3.2}$$

Unless stated otherwise, it is assumed that $\varphi \in C_0^\infty$. For (3.2) to define Λf as a distribution, it is necessary to impose a condition on f at ∞. For the purposes of this article, a convenient condition is

$$f(1+|x|)^{-1-n} \in L^1. \tag{3.3}$$

For $n \geqq 2$, the Riesz kernel R_1 is defined by

$$\begin{aligned} &R_1(x) = (1/(\pi|S^{n-2}|))|x|^{1-n}, \quad \text{with} \\ &\partial R_1/\partial x_j = -(n-1)(1/(\pi|S^{n-2}|))x_j|x|^{-1-n}. \end{aligned} \tag{3.4}$$

The convolution

$$R_1 * f(x) = \int R_1(x-y)f(y)\,dy \tag{3.5}$$

exists (as an absolutely convergent integral) for at least one x if and only if $f(1+|x|)^{1-n} \in L^1$; if this is the case, then $R_1 * f$ exists almost everywhere and is locally integrable. The Cauchy principal value convolution is defined by

$$\text{v.p.}\partial R_1/\partial x_j * f(x) = \lim_{\varepsilon\to 0} \int_{|y|>\varepsilon} \partial R_1/\partial x_j(y) f(x-y)\,dy. \tag{3.6}$$

By the Calderón-Zygmund theory of singular integrals, if $f \in L^p$, $1<p<\infty$, the limit in (3.6) exists almost everywhere and in L^p, and the resulting function is in L^p.

The Fourier transform of R_1 is

$$\hat{R}_1(\xi) = (2\pi)^{-n/2}|\xi|^{-1}. \tag{3.7}$$

From (3.1) and (3.7) it follows that

$$\Lambda^{-1}\varphi(x) = R_1 * \varphi(x) = \int R_1(x-y)\varphi(y)\,dy. \tag{3.8}$$

Hence

$$\Lambda\varphi(x) = -R_1 * \Delta\varphi(x) = -\int R_1(x-y)\Delta\varphi(y)\,dy. \tag{3.9}$$

By the Calderón-Zygmund theory, for $\varphi \in H^1$,

$$\Lambda\varphi(x) = -\textstyle\sum_1^n \text{v.p.}\partial R_1/\partial x_j * \partial\varphi/\partial x_j. \tag{3.10}$$

THEOREM 3.11. *If* $f(1+|x|)^{-1-n} \in L^1$, *the formula* $\langle \Lambda f, \varphi \rangle = \langle f, \Lambda \varphi \rangle$ *defines* Λf *as a tempered distribution. If* $f(1+|x|)^{-s} \in L^2$, $s < (n+2)/2$, *then* $(\Lambda f)\hat{} = |\xi|\hat{f}$.

Proof. The Schwartz space S consists of the functions $\varphi \in C^\infty$ such that for each m and N

$$\|\varphi\|_{m,N} = \max\left\{(1+|x|)^N \sum_{|k|\leqq m} |D^k\varphi(x)|\right\} < \infty,$$

the sum being taken over all derivatives of orders $\leqq m$, the maximum over all x. The $\|\varphi\|_{m,N}$ are the seminorms defining the topology. The tempered distributions are the elements of the dual space S', so the assertion of the first part of the theorem is that there exist C, m, and N so that

$$|\langle f, \Lambda\varphi\rangle| = \left|\int f(x)\Lambda\varphi(x)\,dx\right| \leqq C\|\varphi\|_{m,N} \quad \text{for all } \varphi \in S.$$

This (together with the existence of the integral) is proved by showing the existence of C, m, and N so that

$$|\Lambda\varphi(x)| \leqq C\|\varphi\|_{m,N}(1+|x|)^{-1-n} \quad \text{for all } \varphi \in S. \tag{3.12}$$

On $|x| \leqq 2$, such an evaluation is clear, so it will be assumed that $|x| > 2$. By (3.10) $\Lambda\varphi(x)$ is a constant times a sum of terms

$$\lim_{\varepsilon\to 0} \int_{|x-y|>\varepsilon} [(x_j - y_j)|x-y|^{-1-n} - x_j|x|^{-1-n}]\partial\varphi/\partial y_j(y)\,dy,$$

the subtraction of $x_j|x|^{-1-n}$ being allowed because the integral of $\partial\varphi/\partial y_j$ is 0. The integral is evaluated in several pieces. (The subtraction of $x_j|x|^{-1-n}$ is useful in one of the pieces, and immaterial in the others.)

Consider first the range $\varepsilon < |x-y| < 1$. Since $|x| > 2$, $|x-y| < |x|/2$, and $|x|/2 < |y| < 3|x|/2$. Therefore,

$$|\partial\varphi/\partial y_j(y)| \leqq \|\varphi\|_{1,1}(1+|y|)^{-1} \leqq \|\varphi\|_{1,1}(1+|x/2|)^{-1},$$

and the integral involving $x_j|x|^{-1-n}$ has the required evaluation with $\|\varphi\|_{1,1}$. The other part is equal to

$$\int_{|x-y|<1} (x_j - y_j)|x-y|^{-1-n}(\partial\varphi/\partial y_j(y) - \partial\varphi/\partial y_j(x))\,dy,$$

the subtraction of $\partial\varphi/\partial y_j(x)$ being allowed because the integral of $y_j|y|^{-1-n}$ over S^{n-1} is 0. By the mean value theorem,

$$\partial\varphi/\partial y_j(y) - \partial\varphi/\partial y_j(x) = \langle \nabla\partial\varphi/\partial y_j(c), y-x\rangle,$$

where c lies on the segment from x to y, so that

$$|\nabla\partial\varphi/\partial y_j(c)| \leqq \|\varphi\|_{2,n+1}(1+|x/2|)^{-n-1}.$$

The last integral has the required evaluation with $\|\varphi\|_{2,n+1}$.

This takes care of integration over the range $|x-y| < 1$. The range $|x-y| > 1$ is split into the two parts, $|y| < |x|/2$ and $|y| > |x|/2$. If $|x-y| > 1$, the integrand is $\leqq 2|\partial\varphi/\partial y_j(y)| \leqq 2\|\varphi\|_{1,N}(1+|y|)^{-N}$, so the integral over $|y| \geqq |x|/2$ is at most $C\|\varphi\|_{1,N}(1+|x/2|)^{n-N}$. The required evaluation holds for $\|\varphi\|_{1,N}$ with $N = 2n+1$. Finally, let $|x-y| > 1$ and $|y| < |x|/2$ (where the subtraction of $x_j|x|^{-1-n}$ becomes useful). In this case, write

$$(x_j - y_j)|x-y|^{-1-n} - x_j|x|^{-1-n} = x_j(|x-y|^{-1-n} - |x|^{-1-n}) - y_j|x-y|^{-1-n}.$$

The integral involving y_j has the required evaluation for $\|\varphi\|_{1,N}$ with $N > n+1$. To evaluate the integral involving x_j, note that by the mean value theorem

$$\big||x-y|^{-1-n} - |x|^{-1-n}\big| \leqq (n+1)|x/2|^{-2-n}|y|.$$

Thus, the integral has the required evaluation for $\|\varphi\|_{1,N}$ with $N > n+1$. (In all regions but this one, the evaluations above give $|\Lambda\varphi(x)| = O(|x|^{-N})$, for arbitrary N, but this one gives only $O(|x|^{-1-n})$, which, in fact, is all that is true.)

The Fourier transform is an isomorphism of S onto S. Therefore, if g is a tempered distribution, the formula $\langle \hat{g}, \hat{\varphi}\rangle = \langle g, \bar{\varphi}\rangle$ defines a tempered distribution $\hat{g}$, called the Fourier transform of g. The Fourier transform is also an isomorphism of S' onto S'.

Let $f(1+|x|)^{-s} \in L^2$, i.e., $\hat{f} \in H^{-s}$, $s < (n+2)/2$. Since $(1+|x|)^{-1-n+s} \in L^2$, it follows that $f(1+|x|)^{-1-n} \in L^1$, therefore Λf and $(\Lambda f)\hat{}$ are tempered distributions. From (3.12) it follows that if $\varphi \in S$, then $(\Lambda\varphi)\hat{} \in H^s$, and

$$\||\xi|\hat{\varphi}\|_s = \|(\Lambda\varphi)\hat{}\|_s \leqq C\|\varphi\|_{m,N}.$$

Therefore, $|\langle \hat{f}, |\xi|\hat{\varphi}\rangle| \leqq C\|\hat{f}\|_{-s}\|\varphi\|_{m,N}$, and the formula $\langle |\xi|\hat{f}, \hat{\varphi}\rangle = \langle \hat{f}, |\xi|\hat{\varphi}\rangle$ defines $|\xi|\hat{f}$ as a tempered distribution. The assertion of the second part of the theorem is that the Fourier transform of the tempered distribution $(\Lambda f)\hat{}$ is the tempered distribution $|\xi|\hat{f}$, i.e., that $\langle (\Lambda f)\hat{}, \hat{\varphi}\rangle = \langle \hat{f}, |\xi|\hat{\varphi}\rangle$ for $\varphi \in S$.

Let $f_N(x) = f(x)$ if $|f(x)| \leqq N$, 0 otherwise. By definition, (3.12), and L^2 theory,

$$\langle (\Lambda f)\hat{}, \hat{\bar{\varphi}}\rangle = \langle \Lambda f, \bar{\varphi}\rangle = \langle f, \Lambda\bar{\varphi}\rangle = \lim \langle f_N, \Lambda\bar{\varphi}\rangle = \lim \langle \hat{f}_N, |\xi|\bar{\hat{\varphi}}\rangle.$$

It is clear that $(f_N)\hat{} \to \hat{f}$ in H^{-s}, so the limit is $\langle \hat{f}, |\xi|\bar{\hat{\varphi}}\rangle$.

LEMMA 3.13. *Let $f(1+|x|)^{-1-n} \in L^1$. On any open set where f is locally in the Sobolev space H^s [10], Λf is locally in H^{s-1}. On any open set where f is C^∞, Λf is C^∞. On any open set where f is analytic, Λf is analytic. If x is outside the support of f, then*

$$\Lambda f(x) = -((n-1)/(\pi|S^{n-2}|)) \int |x-y|^{-1-n} f(y)\, dy. \tag{3.14}$$

If f has bounded support, $\Lambda f(x) = O(|x|^{-1-n})$ as $|x| \to \infty$.

Proof. All but formula (3.14), and the final statement which is clear from (3.14), come from the fact that Λ is an analytic elliptic operator of order 1. If the support of φ is disjoint from the support of f, then, by (3.9),

$$\langle \Lambda f, \varphi\rangle = \langle f, \Lambda\varphi\rangle = -\int\int f(x)\Delta R_1(x-y)\varphi(y)\, dy\, dx.$$

This is the scalar product of the right side of (3.14) with φ.

LEMMA 3.15. *Let $f(1+|x|)^{1-n} \in L^1$. $R_1 * f$ is defined almost everywhere as an absolutely convergent integral and is locally integrable. On any open set where f is locally in H^s, $R_1 * f$ is locally in H^{s+1}. On any open set where f is C^∞, $R_1 * f$ is C^∞. On any open set where f is analytic, $R_1 * f$ is analytic. If $f \in L^p$, $p > n$, $R_1 * f$ is continuous. If f has bounded support, $R_1 * f(x) = O(|x|^{1-n})$ as $|x| \to \infty$.*

Proof. The only statement requiring proof is the one about L^p. Fix r, with the aim of proving continuity on $|x| < r$. Let $f' = f$ for $|x| < r$, $f' = 0$ for $|x| > r$. Since $R_1 * (f - f')$ is analytic on $|x| < r$, it is enough to treat $R_1 * f'$. Let $R' = R_1$ for $|x| < 2r$, $R' = 0$ for $|x| > 2r$. Then $R_1 * f' = R' * f'$ on $|x| < r$. If $p > n$ and $(1/p) + (1/p') = 1$, then $p' < n/(n-1)$, and $R' \in L^{p'}$. It is well known (and not hard to verify) that the convolution of a function in L^p with a function in $L^{p'}$ is continuous.

4. General sets and sets with a cone condition. As usual, X is a measurable set in R^n, $n \geqq 2$. When X is the ball with center 0 and radius r, i.e., $X = B(0, r)$, χ_X is usually written as χ_r.

The following formulas result from (3.14) and the observation that $\Lambda(1-f)=\Lambda 1-\Lambda f=-\Lambda f$.

$$\Lambda\chi_X(x)=(n-1)(\pi|S^{n-2}|)^{-1}\int_{X'}|x-y|^{-n-1}\,dy \quad \text{for } x\in X^\circ; \tag{4.1}$$

$$\Lambda\chi_X(x)=-(n-1)(\pi|S^{n-2}|)^{-1}\int_{X}|x-y|^{-n-1}\,dy \quad \text{for } x\in X'^\circ. \tag{4.2}$$

THEOREM 4.3. *Let X and Y be measurable sets.*

(a) *If $f_r(x)=f(x/r)$, then $\Lambda f_r(x)=r^{-1}\Lambda f(x/r)$.*

(b) *$\Lambda\chi_X$ is an analytic function on $(\partial X)'=R^n-\partial X$.*

(c) *$\Lambda\chi_X(x)>0$ on X°, and <0 on X'°; $\Lambda\chi_{X'}=-\Lambda\chi_X$.*

(d) *If $X\subset Y$, then*

$$|\Lambda\chi_X(x)|\geqq|\Lambda\chi_Y(x)| \quad \text{on } X^\circ,$$

$$|\Lambda\chi_X(x)|\leqq|\Lambda\chi_Y(x)| \quad \text{on } Y'^\circ.$$

(e) *If x is not on ∂X, then*

$$\pi d(x,\partial X)|\Lambda\chi_X(x)|\leqq(n-1)|S^{n-1}|/|S^{n-2}|.$$

(f) *If X has finite measure, then, on X'°,*

$$\pi d(x,\partial X)|\Lambda\chi_X(x)|\leqq((n-1)/|S^{n-2}|)|X|d(x,\partial X)^{-n}.$$

Proof. (a) is obvious from the definition. Statements (b), (c), (d), and (f) are immediate from (4.1) and (4.2). To see (e), let $x\in X^\circ$, and let $r=d(x,\partial X)$. The ball B with center x and radius r is contained in X, so, by (d), $\Lambda\chi_r(0)=\Lambda\chi_B(x)\geqq\Lambda\chi_X(x)$. $\Lambda\chi_r(0)$ is evaluated by (4.1). When $x\in X'^\circ$, the proof is the same, with X and X' interchanged.

THEOREM 4.4. *$\Lambda\chi_X$ is subharmonic on X°, and superharmonic on X'°. This implies that*

(a) *$\Lambda\chi_X$ cannot have a local maximum in X°, nor a local minimum in X'°.*

(b) *Fix $a\in X^\circ$. The average of $\Lambda\chi_X$ over the sphere with center a and radius r is an increasing function of r on $0<r<d(a,\partial X)$.*

(c) *Fix a (anywhere). If X is contained in the ball with center a and radius r_0, r^{n-2} times the average of $-\Lambda\chi_X$ over the sphere with center a and radius r is a decreasing function of r on $r>r_0$.*

Proof. $\Delta|x|^{\alpha-n}=(\alpha-n)(\alpha-2)|x|^{\alpha-n-2}>0$ for $\alpha<2$. The statements about sub- and superharmonicity follow from (4.1) and (4.2). Statements (a) and (b) are standard properties of sub- and superharmonic functions. In proving (c), it can be assumed that $a=0$ and $r_0=1$. If g is defined on $|x|>1$, the Kelvin reflection $h(x)=|x|^{2-n}g(x/|x|^2)$ is defined on $|x|<1$ and satisfies $\Delta h(x)=|x|^{-2-n}\Delta g(x/|x|^2)$. Therefore, if g is subharmonic and $O(|x|^{1-n})$, then h is subharmonic on $|x|<1$. The standard mean value property applied to h gives the one stated for g.

When the boundary of X has some smoothness, the inequality in Part (e) of Theorem 4.3 can be sharpened and reversed, with the sharpness depending on the smoothness.

THEOREM 4.5. *If X is a halfspace and x is not on ∂X, then $\pi d(x,\partial X)|\Lambda\chi_X(x)|=1$. If X is convex, $\pi d(x,\partial X)|\Lambda\chi_X(x)|\geqq 1$ on X°, and $\leqq 1$ on X'°.*

Proof. If X is a halfspace, the integrals in (4.1) and (4.2) are evaluated easily by using polar coordinates with center x. If X is convex and $x\in X$, let $\bar{x}$ be a point on ∂X at minimum distance from x. There is a half-space $Y'\subset X'$ with $\bar{x}$ on the boundary.

This half-space is at distance $d(x, \partial X)$ from x, since it cannot intersect the ball with center x and radius $d(x, \partial X)$, the latter being contained in X.

A less sharp inequality holds when X' contains not a halfspace with $\bar{x}$ on the boundary, but only a part of an open cone with vertex $\bar{x}$. Recall (Definition 2.4) that $C(\theta, \alpha, \delta)$ is the open cone with axis θ, opening angle 2α, and radius δ.

THEOREM 4.6. *Let $x \in X^\circ$, and let $\bar{x}$ be a closest point in ∂X to x. If $\bar{x} + C(\theta, \alpha, \delta) \subset X'$, then*

$$\pi d(x, \partial X) \Lambda \chi_X(x) \geqq \left((n-1)/(n|S^{n-2}|)\right)(\delta/(\delta + d(x, \partial X)))^n |S^{n-1} \cap \bar{C}(\theta, \alpha, 1)|.$$

Proof. $\Lambda \chi_X(x) \geqq$ the integral in (4.1) with X' replaced by the cone $\bar{x} + C(\theta, \alpha, \delta)$. This integral is

$$(n-1)(\pi|S^{n-2}|)^{-1} \int_{C(\theta,\alpha,\delta)} |x - \bar{x} - y|^{-n-1}\, dy$$

$$\geqq (n-1)(\pi|S^{n-2}|)^{-1} \int_{C(\theta,\alpha,\delta)} (d(x, \partial X) + |y|)^{-n-1}\, dy,$$

which has the value indicated.

COROLLARY 4.7. *Suppose that there are constants α and δ so that for each $\bar{x} \in \partial X$ there exist θ and θ' with*

$$\bar{x} + C(\theta, \alpha, \delta) \subset X \quad \text{and} \quad \bar{x} + C(\theta', \alpha, \delta) \subset X'.$$

There is a constant c depending only on α and n such that if x is not on ∂X, then

$$c(\delta/(\delta + d(x, \partial X))^n \leqq \pi d(x, \partial X)|\Lambda \chi_X(x)| \leqq (n-1)|S^{n-1}|/|S^{n-2}|.$$

Remark 4.8. If X is bounded and convex with nonempty interior, the conditions of Corollary 4.7 are satisfied. The exterior cone $C(\theta', \alpha, \delta)$ exists with θ' the direction from x to $\bar{x}$, $\alpha = \pi/2$, and $\delta = \infty$. If X contains a ball of radius R and has diameter D, then, for each $\bar{x} \in \partial X$, there is an interior cone $C(\theta, \alpha, \delta)$ with $\alpha = \arcsin(R/D)$ and $\delta = R \cos(\alpha)$.

5. Radial functions. If L is a space of functions, L_0 denotes the subspace of functions with bounded support. If g is a radial function, $\tilde{g}$ is the corresponding even function of one variable. If X is the ball $|x| < r$, $\chi_r = \chi_X$. The dimension n is $\geqq 2$, P (in Theorem 5.2) is defined in formula (A.2), and $E_\theta x = x - \langle x, \theta \rangle \theta$.

LEMMA 5.1. *If the radial $k \in L^p(R^{n-1})$, $p > 2$, then $k(E_\theta x)$ is integrable on S^{n-1}, and*

$$\int_{S^{n-1}} k(E_\theta x)\, d\theta = 2|S^{n-2}| \int_0^{\pi/2} \tilde{k}(|x| \sin(\alpha)) \sin^{n-2}(\alpha)\, d\alpha$$

$$= 2|S^{n-2}||x|^{2-n} \int_0^{|x|} \tilde{k}(t) t^{n-2} (|x|^2 - t^2)^{-1/2}\, dt.$$

Proof. Since $k(E_\theta x) = \tilde{k}((|x|^2 - \langle x, \theta \rangle^2)^{1/2})$, the above equalities hold, provided that the last integral is finite when $\tilde{k}$ is replaced by its absolute value. The condition $k \in L^p$ translates to $\tilde{k} \in L^p$, relative to the measure $t^{n-2}\, dt$. Since $p > 2$, $(|x|^2 - t^2)^{-1/2} \in L^{p'}$, $1/p + 1/p' = 1$, relative to this measure.

THEOREM 5.2. *If* $k \in H_0^s(R^{n-1})$, $s \geqq 0$, *is radial with integral* 0, $k = \Lambda Pe$, *where* $e \in H^{s+1/2}$ *is radial and* $O(|x|^{-n-1})$. *If* $k \in L^p$, $p > 2$,

$$e(x) = (1/\pi) \int_0^{\pi/2} \tilde{k}(|x| \sin(\alpha)) \sin^{n-2}(\alpha)\, d\alpha \tag{5.3}$$

$$= (1/\pi)|x|^{2-n} \int_0^{|x|} \tilde{k}(t) t^{n-2} (|x|^2 - t^2)^{-1/2}\, dt. \tag{5.4}$$

If $k = 0$ *for* $|y| > r$, *then*

$$e(x) = (1/\pi)|x|^{2-n} \int_0^r \tilde{k}(t) t^{n-2} \cdot [(|x|^2 - t^2)^{-1/2} - (|x|^2 - r^2)^{-1/2}]\, dt \quad \text{for } |x| > r. \tag{5.5}$$

Proof. $\hat{k}(\sigma) = h(|\sigma|)$, where h is holomorphic of exponential type. The power series for h contains only even powers, and $h(0) = 0$. Define f on R^n by $\hat{f}(\xi) = (2\pi)^{-1/2} h(|\xi|)/|\xi|^2$. $\hat{f}$ is holomorphic of exponential type, so f has bounded support. Since

$$\int |\xi|^{2s+3} |\hat{f}(\xi)|^2\, d\xi = (2\pi)^{-1} (|S^{n-1}|/|S^{n-2}|) \int |\sigma|^{2s} |\hat{k}(\sigma)|^2\, d\sigma,$$

$f \in H^{s+3/2}$. $e = \Lambda f$ is therefore in $H^{s+1/2}$ and, by Lemma 3.13, is $O(|x|^{-n-1})$. By formulas (3.5) and (9.6) of [7], $\Lambda Pe = k$.

In Theorem A.7, let $f = e_r$, as in (A.14), where e_1 is given by (A.17) with m at least $-1/2$. As $r \to 0$, $e * e_r(x) \to e(x)$ almost everywhere, and $P_\theta e_r * k(y) \to k(y)$ almost everywhere, so it suffices to show that the limit can be placed under the integral. If $H(y)$ is the upper bound of the average of $|k|$ over balls containing y, then $|P_\theta e_r * k(y)| \leqq cH(y)$. By the Hardy-Littlewood maximal theorem, $H \in L^p$, so $H(E_\theta x)$ is integrable over S^{n-1}. (There is a relatively simple proof of the Hardy-Littlewood theorem in [6].)

Formula (5.5), which is useful later, comes from (5.4) and the fact that

$$0 = \int k(x)\, dx = \int \tilde{k}(t) t^{n-2}\, dt.$$

6. Balls. This section contains explicit formulas and precise evaluations of $\Lambda\chi_B$, where B is a ball. These have some interest of their own, and they lead to good evaluations of $\Lambda\chi_X$ for sets X of bounded curvature. Because of the translation invariance and homogeneity, it is enough to discuss the ball with center 0 and radius 1, the characteristic function of which is denoted simply by χ. The dimension n is $\geqq 2$.

By Lemma 3.13, $\Lambda\chi$ is an analytic function on $|x| \neq 1$, and it is $O(|x|^{-1-n})$ as $x \to \infty$. By Lemma 3.11, $\Lambda\chi$ is a tempered distribution on R^n, but, by Theorem 4.5, it is not a (locally integrable) function on any neighborhood of any point on $|x| = 1$. It is shown that on a neighborhood of $|x| = 1$, $\Lambda\chi$ is given by a Cauchy principal value.

In what follows, $e^m = e_1^m$ is the point-spread function defined in (A.17), and $K^m = K_1^m$ is the corresponding local kernel defined in (A.18). Λe^m denotes the distribution defined by $\langle \Lambda e^m, \varphi \rangle = \langle e^m, \Lambda\varphi \rangle$. Note that $\chi = Ce^{-1/2}$.

THEOREM 6.1. *Let* F^m *be the function defined by the right sides of* (5.4) *and* (5.5) *on* $|x| \neq 1$, *with* $k = K^m$. *If* $\operatorname{Re}(m) > -1/2$, $\Lambda e^m = F^m$ *on* R^n. *If* $\operatorname{Re}(m) > -1$, $\Lambda e^m = F^m$ *on* $|x| \neq 1$.

Proof. If $\operatorname{Re}(m) > 1/2$, $k \in L^p$, $p > 2$, and Theorem 5.2 shows that $-\Delta Pe^m = \Lambda PF^m$, from which it follows by the projection-slice theorem ([7], (3.5)]) that $\Lambda e^m = F^m$ on R^n. For $\varphi \in C_0^\infty$, $\langle \Lambda e^m, \varphi \rangle$ is an analytic function on $\operatorname{Re}(m) > -3/2$, while $\langle F^m, \varphi \rangle$ is analytic on $\operatorname{Re}(m) > -1/2$. Since the two are equal on $\operatorname{Re}(m) > 1/2$, they are equal

on $\operatorname{Re}(m) > -1/2$. If φ has support in $|x| \neq 1$, $\langle F^m, \varphi \rangle$ is analytic on $\operatorname{Re}(m) > -1$, so it is equal to $\langle \Lambda e^m, \varphi \rangle$ on $\operatorname{Re}(m) > -1$.

THEOREM 6.2. *Let* $\tilde{k}(t) = 2(1-t^2)^{-3/2}(n-1-(n-2)t^2)$. *On* $|x| \neq 1$ *the distribution* $\Lambda\chi$ *is the function* F *defined by*

$$F(x) = (1/\pi)|x|^{2-n} \int_0^{|x|} \tilde{k}(t) t^{n-2} (|x|^2 - t^2)^{-1/2}\, dt \qquad \text{for } |x| < 1; \tag{6.3}$$

$$F(x) = (1/\pi)|x|^{2-n} \int_0^1 \tilde{k}(t) t^{n-2} [(|x|^2 - t^2)^{-1/2} - (|x|^2 - 1)^{-1/2}]\, dt \qquad \text{for } |x| > 1. \tag{6.4}$$

F *has the form*

$$F(x) = (2/\pi)|x|^{2-n} E(x)(1-|x|^2)^{-1}, \tag{6.5}$$

where E *(given by* (6.8) *below) is continuous and satisfies*

$$|1 - E(x)| \leqq C|1-|x|^2|^{1/2}. \tag{6.6}$$

On R^n, $\Lambda\chi$ *is the principal value* v.p.F *defined by*

$$\langle \text{v.p.}F, \varphi \rangle = \lim_{\varepsilon \to 0} \int_{|1-|x||>\varepsilon} F(x)\varphi(x)\, dx. \tag{6.7}$$

Proof. Theorem 6.1 shows that on $|x| \neq 1$, $\Lambda\chi$ is the function F given by (6.3) and (6.4).

To see that F is as described in (6.5) and (6.6), set $r = |1-|x|^2|^{-1/2}$ and define

$$\tilde{E}_q(|x|) = \int_1^r s^{-2}(1 - s^2/r^2)^{(q-1)/2}(s^2-1)^{-1/2}\, ds, \quad |x| < 1,$$

$$\tilde{E}_q(|x|) = \int_0^r (1 - s^2/r^2)^{(q-1)/2}(s^2+1)^{-1/2}((s^2+1)^{1/2}+1)^{-1}\, ds, \quad |x| > 1$$

$$\tilde{E}_q(1) = \int_1^\infty s^{-2}(s^2-1)^{-1/2}\, ds$$

$$= \int_0^\infty (s^2+1)^{-1/2}((s^2+1)^{1/2}+1)^{-1}\, ds = 1,$$

where q is a nonnegative integer.

With the change of variable $t = (1 - s^2/r^2)^{1/2}$ in (6.3) and (6.4), F assumes the form (6.5) with

$$E(x) = (n-1)E_{n-2}(x) - (n-2)E_n(x). \tag{6.8}$$

An elementary calculation gives

$$\tilde{E}_1(|x|) = |x|, \quad \text{for } |x| < 1,$$

$$\tilde{E}_1(|x|) = (|x| + (|x|^2-1)^{1/2})^{-1} \quad \text{for } |x| > 1.$$

Consider the case $|x| < 1$ and $q = 0$. Since $1 = \tilde{E}_q(1)$,

$$\tilde{E}_0(|x|) - 1 = \int_1^r s^{-2}(1 - s^2/r^2)^{-1/2}(s^2-1)^{-1/2}\, ds$$

$$- \int_1^r s^{-2}(s^2-1)^{-1/2}\, ds - \int_r^\infty s^{-2}(s^2-1)^{-1/2}\, ds$$

$$= \int_1^r (s^2-1)^{-1/2}(r + (r^2-s^2)^{1/2})^{-1}(r^2-s^2)^{-1/2}\, ds + \tilde{E}_1(|x|) - 1.$$

Let $r>2$. If $1\leqq s\leqq r/2$ the integrand is $\leqq r^{-2}(s^2-1)^{-1/2}$, so the integral over this range is $\leqq r^{-2}\log(r)$. If $r/2\leqq s\leqq r$ the integrand is $\leqq 2r^{-1}(r^2-4)^{-1/2}(r^2-s^2)^{-1/2}$, so the integral over this range is $\leqq(2\pi/3)r^{-1}(r^2-4)^{-1/2}$. Therefore,

$$|\tilde{E}_0(|x|)-1|\leqq C(1-|x|^2)\log(2/(1-|x|^2)) \quad \text{for all } |x|<1. \tag{6.9}$$

If q is an integer $\geqq 2$ (still $|x|<1$),

$$1-\tilde{E}_q(|x|)=(1/r)\sum_0^{q-2}\int_1^r (s^2-1)^{-1/2}(r+(r^2-s^2)^{1/2})^{-1}(1-s^2/r^2)^{p/2}\,ds+1-\tilde{E}_1(|x|).$$

Since $0\leqq 1-s^2/r^2\leqq 1$, evaluations like the ones above give

$$|\tilde{E}_q(|x|)-\tilde{E}_q(1)|\leqq C(1-|x|^2)\log(2/(1-|x|^2)), \quad |x|<1 \tag{6.10}$$

for all nonnegative integers q, $|x|<1$.

For $|x|>1$, similar but simpler evaluations give

$$|\tilde{E}_q(|x|)-1|\leqq C|1-|x|^2|^{1/2}. \tag{6.11}$$

Consequently, (6.6) holds for all x.

This shows that F is as described in (6.3)-(6.6). The next step is to show that the limit in (6.7) exists.

Since f is radial, it can be assumed that φ is radial. By (6.5) and (6.6),

$$F(x)=(2/\pi)|x|^{2-n}(1-|x|^2)^{-1}+G(x), \quad \text{with } G \text{ locally integrable.}$$

Therefore

$$\begin{aligned}\langle \text{v.p.}F,\varphi\rangle &= (1/\pi)|S^{n-1}|\lim_{\varepsilon\to 0}\int_{|1-|s||>\varepsilon}|s|(1-s^2)^{-1}\tilde{\varphi}(s)\,ds \\ &\quad +(1/2)|S^{n-1}|\int |s|^{n-1}\tilde{G}(s)\tilde{\varphi}(s)\,ds \\ &= (1/\pi)|S^{n-1}|\langle \text{v.p.}(1-s)^{-1},\tilde{\varphi}\rangle+\langle g,\tilde{\varphi}\rangle,\end{aligned} \tag{6.12}$$

where $\text{v.p.}(1-s)^{-1}$ is the Cauchy principal value of $(1-s)^{-1}$, and g is an even locally integrable function. This shows that the principal value defined in (6.7) exists.

Since $\text{v.p.}F=F$ on $|x|\neq 1$, it follows that

$$\Lambda\chi=\text{v.p.}F+D, \tag{6.13}$$

where D is a radial distribution with support on $|x|=1$. It remains to show that $D=0$.

Standard formulas for Bessel functions give

$$(\Lambda\chi)\hat{}\,(\xi)=|\xi||\xi|^{-n/2}J_{n/2}(\xi)=O(|\xi|^{-(n-1)/2}).$$

Therefore, $\Lambda\chi\in H^{-s}$ for $s>1/2$, and

$$|\langle\Lambda\chi,\varphi\rangle|\leqq C\|\varphi\|_s \quad \text{for } s>1/2. \tag{6.14}$$

It is easy to see that if φ is radial and 0 for $|x|>R$, then

$$\|\varphi\|_0\leqq CR^{(n-1)/2}\|\tilde{\varphi}\|_0 \quad \text{and} \quad \|\varphi\|_1\leqq CR^{(n-1)/2}\|\tilde{\varphi}\|_1.$$

Interpolation gives

$$\|\varphi\|_s\leqq CR^{(n-1)/2}\|\tilde{\varphi}\|_s \quad \textit{for } 0\leqq s\leqq 1, \tag{6.15}$$

then (6.14) gives

$$|\langle \Lambda\chi, \varphi\rangle| \leqq CR^{(n-1)/2}\|\tilde{\varphi}\|_s \quad \text{for } 1/2 < s \leqq 1. \tag{6.16}$$

This implies that the even distribution $(\Lambda\chi)^{\sim}$ defined by

$$\langle (\Lambda\chi)^{\sim}, \tilde{\varphi}\rangle = \langle \Lambda\chi, \varphi\rangle \tag{6.17}$$

lies in H^{-s} locally for $s > 1/2$.

Let $\tilde{\varphi}$ be even and equal to 1 on a neighborhood of 1. From (6.13) and (6.12), it follows that

$$\tilde{\varphi}\Lambda\chi = (1/\pi)|S^{n-1}|\tilde{\varphi}\,\text{v.p.}(1-s)^{-1} + g + \tilde{D}, \tag{6.18}$$

where g is integrable and $D^{\sim}$ has support at 1, so it is a linear combination of derivatives of δ. All terms but $D^{\sim}$ lie in H^{-s} for $s > 1/2$, so D does, too. Therefore, $D^{\sim}$ cannot involve derivatives of δ, but only δ itself. The fact that $D = 0$ is a consequence of the following lemmas, in which $e \in C^{\infty}$ is radial, $e = 0$ for $|x| \geqq 1$, and the integral of e is 1; and $H = F - G$ with $G(x) = (2/\pi)|x|^{2-n}(1-|x|^2)^{-1}$.

LEMMA 6.19. *If $c > 0$, $c \neq 1$, and $e_r(x) = r^{-n}e(x/r)$,*

$$\lim_{r\to 0}\langle \text{v.p.}G, e_r * \chi_c\rangle = (-1/2)|S^{n-1}|\log|1-c^2|. \tag{6.20}$$

Proof. Let $G_\varepsilon(x) = G(x)$ for $|1-|x|| \geqq \varepsilon$, $= 0$ otherwise, so that $\langle \text{v.p.}G, e_r * \chi_c\rangle$ is the limit as $\varepsilon \to 0$ of $\langle G_\varepsilon, e_r * \chi_c\rangle$.

Consider first $c < 1$. If $r < 1-c$, then on $|y| > c+r$ and $|x| < r$, $|x-y| > c$, and $e_r * \chi_c(y) = 0$. If $\varepsilon < 1-r-c$, then

$$\langle G_\varepsilon, e_r * \chi_c\rangle = \int_{|y|<c+r} G(y)e_r * \chi_c(y)\,dy. \tag{6.21}$$

The right side is independent of ε, and as $r \to 0$ it approaches

$$\int_{|y|<c} G(y)\,dy = |S^{n-1}|\int_0^c s(1-s^2)^{-1}\,ds = (-1/2)|S^{n-1}|\log|1-c^2|. \tag{6.22}$$

Consider now $c > 1$. If $r < c-1$, then on $|y| < c-r$ and $|x| < r$, $|x-y| < c$, and $e_r * \chi_c(y) = 1$. If $\varepsilon < c-r-1$, then

$$\langle G_\varepsilon, e_r * \chi_c\rangle = \int_{|y|<c-r} G_\varepsilon(y)\,dy + \int_{|y|>c-r} G(y)\,e_r * \chi_c(y)\,dy.$$

As $\varepsilon \to 0$, the first integral has the limit

$$(-1/2)|S^{n-1}|\log|1-(c-r)^2|.$$

The second, which is independent of ε has limit 0 as $r \to 0$.

LEMMA 6.23. *The limit as $r \to 0$ of $\langle \Lambda\chi, e_r * \chi_c\rangle$ is*

$$\int_{|y|<c} F(y)\,dy \quad \text{if } c < 1, \qquad \int_{|y|<1/c} F(y)\,dy \quad \text{if } c > 1.$$

Proof. If $c < 1$ and $r < 1-c$, the support of $e_r * \chi_c$ does not meet $|x| = 1$, so $\langle \Lambda\chi, e_r * \chi_c\rangle = \langle F, e_r * \chi_c\rangle$, which approaches the integral indicated.

For each x,

$$\Lambda(e_r * \chi_c)(x) = (\Lambda\, e_r * \chi_c)(x) = \langle \Lambda\, e_r(x\text{-}.), \chi_c\rangle = \langle e_r(x\text{-}.), \Lambda\chi_c\rangle.$$

If $c>1$ and $r<c-1$, on $|x|\leqq 1$ the support of $e_r(x\text{-}.)$ does not meet $|y|=c$, so, by part (a) of Theorem 2.1,

$$\langle \chi, \Lambda(e_r * \chi_c)\rangle = (1/c)\int\int \chi(x)\, e_r(x-y)F(y/c)\, dy\, dx,$$

which approaches the integral indicated.

The proof that $D=0$ is finished as follows. Let

$$\begin{aligned} &f_\delta = \chi_{1+\delta} - \chi_{1-\delta}, \\ &\langle \Lambda\chi, e_r * f_\delta\rangle = \langle \text{v.p.}G, e_r * f_\delta\rangle + \langle H, e_r * f_\delta\rangle + \langle D, e_r * f_\delta\rangle \end{aligned} \tag{6.24}$$

and take the limit, first as $r\to 0$, then as $\delta\to 0$. By Lemma 6.23 and formula (6.22), the limit on the left as $r\to 0$ is $(-1/2)|S^{n-1}|\log(2+\delta)/((2-\delta)(1+\delta)^2)$ plus the integral of H over $1-\delta<|y|<1/(1+\delta)$. Both terms go to 0 as $\delta\to 0$. Thus, the left side of (6.24) $\to 0$ as $\delta\to 0$. By Lemma 6.19, as $r\to 0$, $\langle \text{v.p.}G, e_r * f_\delta\rangle$ goes to $(-1/2)|S^{n-1}|\cdot\log((2+\delta)/(2-\delta))$, which goes to 0 as $\delta\to 0$. $\langle H, e_r * f_\delta\rangle$ goes to $\langle H, f_\delta\rangle$ as r goes to 0, then to 0 as $\delta\to 0$. On the other hand,

$$\langle D, \varphi\rangle = c\int_{S^{n-1}} \varphi(\theta)\, d\theta;$$

so, for $r<\delta$, $\langle D, e_r * f_\delta\rangle = c|S^{n-1}|$, and c must be 0.

7. Sets of bounded curvature.

DEFINITION 7.1. X has curvature $\leqq 1/r$ along a subset X_0 of ∂X if for each point $\bar{x}\in X_0$ there are open balls $B\subset X$ and $B'\subset X'$ of radius r with $\bar{x}\in \bar{B}\cap\bar{B}'$.

Let

$$E_1(x) = 2|x|^{2-n}(1+|x|)^{-1}E(x) \tag{7.2}$$

with E as in Theorem 6.2. For $|x|\neq 1$,

$$\Lambda\chi(x) = (1/(\pi(1-|x|)))E_1(x) \quad\text{and}\quad |1-E_1(x)|\leqq C|1-|x||^{1/2}. \tag{7.3}$$

THEOREM 7.4. *Let X have curvature $\leqq 1/r$ along X_0. If $x\in R^n-\partial X$, and $d(x, X_0) = d(x,\partial X)<r$, then*

$$\tilde{E}_1(1+(d(x,\partial X)/r))\leqq \pi|\Lambda\chi_X(x)|\, d(x,\partial X)\leqq \tilde{E}_1(1-(d(x,\partial X)/r)), \tag{7.5}$$

$$\big||\Lambda\chi_X(x)| - (1/(\pi d(x,\partial X))\big|\leqq Cr^{-1/2}\, d(x,\partial X)^{-1/2}. \tag{7.6}$$

Proof. Let $x\in X^\circ$, and let $\bar{x}$ be a point in X_0 with $|x-\bar{x}| = d(x,\partial X)$. Let B'' be the ball with center x and radius $|x-\bar{x}|$. $\bar{B}'\cap\bar{B}''$ is not empty, since both contain $\bar{x}$. If x is not on the line joining $\bar{x}$ to the center c' of B', then $B'\cap B''$ is not empty, which is impossible, since $B'\subset X'$ and $B''\subset X$. Similarly, the center c of B is on this same line. Therefore,

$$|x-c| = r - d(x,\partial X), \tag{7.7}$$

and $x\in B$. By Theorem 4.3,

$$|\Lambda\chi_{B'}(x)|\leqq|\Lambda\chi_X(x)|\leqq|\Lambda\chi_B(x)| = (1/r)|\Lambda\chi((x-c)/r).$$

The right-hand inequality in (7.5) comes from putting (7.7) into the left formula in (7.3). $\Lambda\chi_{B'}$ is treated similarly, the only difference being that $|x-c'| = r+d(x,\partial X)$.

When $x\in X'$, the evaluations are the same with the roles of B and B′ reversed.

The inequality (7.6) comes from the right inequality in (7.3).

8. Λ^{-1}: convolution with R_1. Since $R_1 * f$ is defined only when $f(1+|x|)^{1-n} \in L^1$, the interplay between a set X and its complement X' is no longer available. Throughout the section, X and Y are bounded measurable sets in R^n, $n \geqq 2$.

THEOREM 8.1.

(a) $R_1 * \chi_X$ is continuous on R^n, analytic on $R^n - \partial X$, and subharmonic on X'°.

(b) If $X \subset Y$, then $R_1 * \chi_X(x) \leqq R_1 * \chi_Y(x)$ for all x.

(c) If X has diameter δ, $R_1 * \chi_X(x) \leqq \delta |S^{n-1}|/(\pi |S^{n-2}|)$.

(d) For $x \in X'$, $R_1 * \chi_X(x) \leqq (|X|/(\pi |S^{n-2}|))\, d(x, \partial X)^{1-n}$.

Proof. Statements (a), (b), and (d) are obvious. In proving (c), first let $x \in X^\circ$. Then the ball B with center x and radius δ contains X, so by (b), $R_1 * \chi_X(x) \leqq R_1 * \chi_B(x)$, which is easily seen to have the value shown. Since $R_1 * \chi_X$ is continuous, the inequality holds on $\bar{X}$. Since $R_1 * \chi_X$ is subharmonic on X'°, and the inequality holds on the boundary, it holds throughout X'°.

As before, reverse inequalities come from rather explicit information about balls. If $g(x) = f(x/r)$, then $R_1 * g(x) = rR_1 * f(x/r)$, so it is sufficient to treat the unit ball with characteristic function χ.

THEOREM 8.2.

$$R_1 * \chi(x) = (2/\pi) \int_0^1 (1-|x|^2 t^2)^{1/2} t^{n-2} (1-t^2)^{-1/2}\, dt \quad \textit{for } |x| < 1,$$

$$R_1 * \chi(x) = (2/\pi)|x|^{2-n} \int_0^1 (1-t^2)^{1/2} t^{n-2} (|x|^2 - t^2)^{-1/2}\, dt \quad \text{for } |x| > 1.$$

$R_1 * \chi$ is a positive decreasing function of $|x|$. It is a concave function of $|x|$ on $|x| < 1$, and a convex function of $|x|$ on $|x| > 1$.

Proof. By formula (A.6),

$$R_1 * f(x) = (1/(2\pi |S^{n-2}|)) \int_{S^{n-1}} P_\theta f(E_\theta x)\, d\theta.$$

The two formulas follow from this and Lemma 5.1, and the fact that $P_\theta \chi(y) = 2(1-|y|^2)^{1/2}$, $|y| < 1$. The last statements are obtained by differentiating these formulas.

THEOREM 8.3. *Let $x \in R^n - \partial X$, let $\bar{x}$ be a point on ∂X at minimum distance from x, and let r be the radius of the largest ball B contained in X, with center on the line joining x and $\bar{x}$ and with $\bar{x} \in \bar{B}$. If $C = (n-1)|S^{n-1}|/|S^{n-2}|$, then*

$$(n-1)\pi R_1 * \chi_X(x) \geqq (C-2) d(x, \partial X) + 2r \quad \textit{for } x \in X^\circ,$$

$$(n-1)\pi R_1 * \chi_X(x) \geqq C(r/n)(1+(d(x, \partial X)/r))^{1-n} \quad \textit{for } x \in X'^\circ.$$

Proof. If c is the center of B, then by Theorem 8.1,

$$R_1 * \chi_X(x) \geqq R_1 * \chi_B(x) = rR_1 * \chi((x-c)/r).$$

If $x \in X^\circ$, then $|x-c| = r - d(x, \partial X)$, the last quantity is

$$r(R_1 * \chi)\tilde{}\,(1-(d(x, \partial X)/r)),$$

and the proof of the first inequality is finished by evaluating $(R_1 * \chi)\tilde{}$ at 0 and 1, and using the concavity. Now, $R_1 * \chi_B(x)$ is $|S^{n-1}|r^n/n$ times the average of $R_1(x-y)$ over

B. If $x \in X'^{\circ}$, then $R_1(x-y)$ is subharmonic on B, so the average is $\geqq R_1(x-c)$, the value at the center of B. In this case, $|x-c| = r + d(x, \partial X)$.

9. Dimension 2. In dimension 2 the reconstruction integrals in formulas (A.9) and (A.12) are usually carried out in terms of the variables α, φ, and τ (the latter depending on α) defined by

$$\begin{aligned} &a = R\,(\cos(\alpha), \sin(\alpha)),\ \theta = -(\cos(\alpha-\varphi), \sin(\alpha-\varphi)), \\ &x - a = -|x-a|(\cos(\alpha-\tau), \sin(\alpha-\tau)). \end{aligned} \tag{9.1}$$

With these variables (A.9) and (A.12) become

$$e * f(x) = (1/4\pi) \int_0^{2\pi} \int_{-\pi/2}^{\pi/2} D_\alpha f(\varphi) \cos(\varphi) k(|x-a| \sin(\tau-\varphi))\, d\varphi\, d\alpha, \tag{9.2}$$

$$\Lambda e * f(x) = (R/4\pi) \int_0^{2\pi} \int_{-\pi/2}^{\pi/2} D_\alpha f(\varphi) \cos(\varphi) K(|x-a| \sin(\tau-\varphi))\, d\varphi\, d\alpha. \tag{9.3}$$

These formulas require evaluation of the inner integral at each point x of the two-dimensional reconstruction matrix. In order to avoid excessive computation, Lakshminarayanan devised the ingenious "homogeneous approximation." With $K = K_r$, as defined in (A.16),

$$K(|x-a| \sin(\tau-\varphi)) = |x-a|^{-3} K_s(\sin(\tau-\varphi)), \quad s = r/|x-a|.$$

The approximation consists in replacing $s = r/|x-a|$ by a constant s independent of x and a. With this approximation (9.3) becomes

$$\Lambda e_r * f(x) \sim (R/4\pi) \int_0^{2\pi} |x-a|^{-3} \int_{-\pi/2}^{\pi/2} D_\alpha f(\varphi) \cos(\varphi) K_s(\sin(\tau-\varphi))\, d\varphi\, d\alpha. \tag{9.4}$$

The inner integral can now be computed for a set of equidistant values of τ, and extended to others by interpolation, the point being to remove the dependence on x and a. The reconstructions of the resolution phantom, head, and abdomen shown in § 2 come from an implementation of (9.4), with a global Shepp-Logan kernel for the standard reconstructions.

The exact consequences of the Lakshminarayanan approximation are not known. It has proved remarkably effective when the x-ray sources are not too close to the object, e.g., on a circle of radius ~2.5 for an object contained in a circle of radius 1. In the case of local tomography, some insight can be obtained by evaluating the limit of the inner integral in (9.3) as the point spread radius goes to 0.

For fixed x and a, hence fixed α and τ, let $I(x, a)$ denote the inner integral in (9.3), with $K = K_r = -(Pe_r)''$. If $g(\varphi) = D_\alpha(\varphi)$, and $t = -|x-a| \sin(\tau-\varphi)$,

$$I(x, a) = -\int_{-c}^{c} g(\varphi) \cos(\varphi) \varphi'(Pe_r)''\, dt, \quad c = |x-a| \cos(\tau).$$

Since $g(\varphi)$ vanishes near $\pm\pi/2$, integration by parts gives

$$I(x, a) = -\int_{-c}^{c} (g(\varphi) \cos(\varphi) \varphi')'' Pe_r\, dt.$$

As $r \to 0$, $Pe_r \to \delta$, so

$$\lim_{r\to 0} I(x, a) = -(g(\varphi)\cos(\varphi)\varphi')''(0) \tag{9.5}$$
$$= -|x-a|^{-3}(\cos(\tau)g''(\tau) - 2\sin(\tau)g'(\tau)).$$

Formula (9.3) gives

$$\Lambda f(x) = -(R/4\pi)\int_0^{2\pi} |x-a|^{-3}(\cos(\tau)(D_\alpha f)''(\tau) - 2\sin(\tau)(D_\alpha f)'(\tau))\, d\alpha \tag{9.6}$$
$$= -(R/4\pi)\int_0^{2\pi} |x-a|^{-3}(1+d^2/d\tau^2)(\cos(\tau)D_\alpha f(\tau))\, d\alpha.$$

In this setting, the approximate reconstruction formula (9.4) appears as a natural basis for discretizing the exact formula (9.6): the operator $-(1+d^2/d\tau^2)$ is approximated by convolution with $K_s(\sin(\tau))$.

It has been observed empirically that cup artifacts beyond the intrinsic ones occur unless the sum of the discrete kernel values is very small relative to the kernel maximum. Viewing the convolution as an approximation to $-(1+d^2/d\tau^2)$ provides an intuitive explanation. A kernel discretizing $d^2/d\tau^2$ should have mean value ~ 0 relative to a kernel maximum of size h^{-2}, where h is the step size. Thus a discrete kernel for $-(1+d^2/d\tau^2)$ should have a mean value of size 1 relative to a kernel maximum of size h^{-2}. With equidistant sampling, the exponent $m = 11.4174$ provides such a discrete kernel when r is chosen so that the kernel minimum falls on any of the first three detectors. The importance of kernel sum 0 in parallel beam sampling is discussed in [1].

Appendix. Reconstruction formulas. The divergent and parallel beam x-ray transforms of a function f on R^n are defined by

$$Df(a, \theta) = D_a f(\theta) = \int_0^\infty f(a+t\theta)\, dt, \quad \theta \in S^{n-1}, \tag{A.1}$$

$$Pf(\theta, x) = P_\theta f(x) = \int_{-\infty}^\infty f(x+t\theta)\, dt, \quad x \in \theta^\perp. \tag{A.2}$$

A useful auxiliary operator is

$$L_a f(y) = D_a f(y/|y|) + D_a f(-y/|y|). \tag{A.3}$$

The x-ray attenuation coefficient f is assumed to be square integrable with support in $|x| \le 1$. $D_a f(\theta)$ is the attenuation along the ray with origin a (the x-ray source) and direction θ. It is assumed that the x-ray sources lie on a sphere A of radius $R > 1$. $P_\theta f(x)$ is the attenuation along the line through x with direction θ. $L_a f(x-a)$ is the attenuation along the line joining x and a.

Inversion formulas are obtained easily. Indeed,

$$\int_{S^{n-1}} D_a f(\theta)\, d\theta = \int_{S^{n-1}}\int_0^\infty f(a+t\theta)\, dt\, d\theta = \int f(a+x)|x|^{1-n}\, dx, \tag{A.4}$$

so (with Λ applied to the integral as a function of a)

$$f(a) = (1/(\pi|S^{n-2}|))\Lambda\int_{S^{n-1}} D_a f(\theta)\, d\theta. \tag{A.5}$$

Since $D_a f(\theta) + D_a f(-\theta) = P_\theta f(E_\theta a)$, where E_θ is the orthogonal projection on $\theta^\perp$, formula (A.5) gives

$$f(a) = (1/(2\pi|S^{n-2}|))\Lambda \int_{S^{n-1}} P_\theta f(E_\theta a)\, d\theta. \tag{A.6}$$

Because of the singularities in Λ (differentiation and singular integration), numerical evaluations require the use of approximate formulas. In practice, these usually are formulas for $e * f$, where e is an approximate δ-function.

The general approximate inversion formulas, proved in [9], are as follows (with H^s, the Sobolev space of order s):

THEOREM A.7. *If* $e \in H^{1/2}$, $(1+|x|)^{1-n} e \in L^1$, *and* $\hat{e}/|\xi| \in L^1_{\text{loc}}$ *then, with* $k = \Lambda P e$

$$e * f(x) = (1/(2\pi|S^{n-2}|)) \int_{S^{n-1}} P_\theta f * k(E_\theta x)\, d\theta, \tag{A.8}$$

$$e * f(x) = (1/(4\pi R|S^{n-2}|)) \int_A \int_{S^{n-1}} L_a f(\theta) |\langle a, \theta\rangle| k(E_\theta(x-a))\, d\theta\, da. \tag{A.9}$$

Formula (A.9) comes from formula (A.8) and the following [8]:

$$P_\theta f * g(E_\theta x) = (1/2R) \int_A L_a f(\theta) |\langle a, \theta\rangle| g(E_\theta(x-a))\, da. \tag{A.10}$$

In ordinary tomography the "point-spread function" e is an approximate delta function, and $e * f$ is an approximation to f. Such formulas were introduced by Lakshminarayanan [3] with the point-spread function $e(x) = (1/2)J_1(|x|)/|x|$ in dimension $n = 2$.

In local tomography, introduced in [9] and [12], e is replaced by Λe, in which case, since $\Lambda^2 = -\Delta$, Theorem A.7 becomes

THEOREM A.11. *If* $e \in H^{3/2}$ *and* $(1+|x|)^{1-n} \Lambda e \in L^1$, *then, with* $K = -\Delta P e$,

$$\Lambda e * f(x) = 1/(4\pi R|S^{n-2}|) \int_A \int_{S^{n-1}} L_a f(\theta) |\langle a, \theta\rangle| K(E_\theta(x-a))\, d\theta\, da. \tag{A.12}$$

Formally, $\Lambda e * f = e * \Lambda f$. If e is an approximate δ-function, $\Lambda e * f$ becomes an approximation to Λf, which is very different from f, but has the same singularities, since Λ is an elliptic pseudodifferential operator. (The local tomography in [12] is based on a different approximation to Δ.)

Ordinary tomography is global because the kernel k in Theorem A.7 cannot have bounded support. $\hat{k}(\xi) = (2\pi)^{1/2}|\xi|\hat{e}(\xi)$, with $\hat{e}(0) \neq 0$, so $\hat{k}$ cannot be analytic. If the point-spread function e has bounded support, it normally has very small support, and the kernel K in Theorem A.11 has equally small support. Therefore, the tomography of Theorem A.11 is local. The value of $\Lambda e * f(x)$ is obtained from attenuation measurements along rays passing very close to x (within a millimeter or so, on a medical scale). Moreover, the inner integral in (A.12) requires only some 3–8 multiplications (depending on the noise.)

To compute the countercups described in §§ 2 and 8, it is necessary to have a formula for $R_1 * f$ where the integration takes place over the source sphere A, rather

than the detector sphere S^{n-1}. This can be obtained from the symmetry relation $L_x f(a-x) = L_a f(x-a)$. By (A.5), with $C_n = 1/(\pi|S^{n-2}|)$

$$R_1 * f(x) = C_n \int_{S^{n-1}} D_x f(\theta)\, d\theta = (1/2) C_n \int_{S^{n-1}} L_x f(\theta)\, d\theta.$$

For fixed x either inside or outside (but not on) the source sphere A, let $\theta = (a-x)/|a-x|$. The symmetry relation gives

$$R_1 * f(x) = (1/2) C_n \int_{S^{n-1}} L_a f(x-a)\, d\theta.$$

With the change of variable $\theta = (a-x)/|a-x|$,

$$d\theta = R^{-1} |\langle x-a, a\rangle| |x-a|^{-n}\, da,$$

so the result is

$$R_1 * f(x) = (1/2R) C_n \int_A L_a f(x-a) |\langle x-a, a\rangle| |x-a|^{-n}\, da. \tag{A.13}$$

Remark. When the point x is outside the source sphere A, the map $a \to \theta$ is neither 1-1 nor onto.

The usual way to get point-spread functions and kernels is to fix an initial function e_1 with $\hat{e}_1$ bounded and continuous at 0, and with $\hat{e}_1(0) = (2\pi)^{-n/2}$ (or integral $e_1 = 1$ if e_1 is integrable). If

$$e_r(x) = r^{-n} e_1(x/r), \tag{A.14}$$

then, as $r \to 0$, $e_r * f \to f$ in various senses, depending on additional properties of e_1 and f. For small r, e_r is an approximate δ-function. If k_1 is the global tomography kernel corresponding to $e_1 (k_1 = \Lambda P e_1)$, then

$$k_r(y) = r^{-n} k_1(y/r) \tag{A.15}$$

is the kernel corresponding to e_r. If K_1 is the local tomography kernel corresponding to $e_1 (K_1 = -P\Delta e_1)$, then

$$K_r(y) = r^{-n-1} K_1(y/r) \tag{A.16}$$

is the local kernel corresponding to e_r. The choice of r depends primarily on the nature of e_1, the resolution required, and the noise. See [2].

The original point-spread function is the one of Ram-Lak [4]. One in widespread current use is that of Shepp-Logan [5]. Point-spread functions useful for both global and local tomography [2], [8], [9] are the functions

$$\begin{aligned} e_1^m(x) &= C(1-|x|^2)^{m+1/2} \quad \text{for } |x|<1, \quad = 0 \text{ for } |x|>1, \\ &(C = \Gamma((2m+3+n)/2)/\pi^{n/2}\Gamma((2m+3)/2)). \end{aligned} \tag{A.17}$$

The corresponding global kernel has a complicated analytic expression, but a very quickly convergent series expansion [8]. The corresponding local kernel $(K_1 = -\Delta P e_1)$ is

$$\begin{aligned} &K_1^m(y) = C(1-|y|^2)^{m-1}(n-1-(2m+n-1)|y|^2) \quad \text{for } |y|<1, \\ &C = 2\Gamma((2m+3+n)/2)/\pi^{(n-1)/2}\Gamma(m+1). \end{aligned} \tag{A.18}$$

In practice, we use this local kernel with $m = 11.4174$. e_r^m and K_r^m, with m complex, are also useful in the computation of $\Lambda\chi_r$, where χ_r is the characteristic function of the ball $B(0, r)$ because χ_r is a multiple of $e_r^{-1/2}$.

Remark. The proofs in [9] of Theorems A.7 and A.11 made use of the fact that if φ is in the Schwartz space S of rapidly decreasing C^∞ functions and $\varphi(0) = 0$, then

$$\varphi(x) = \sum_1^n x_j \varphi_j \quad \text{with } \varphi_j \in S. \tag{A.19}$$

The proof in [9] is incomplete.

Proof. For fixed x, integration of the derivative of $\varphi(tx)$ gives

$$\varphi(x) = -\sum_1^n x_j \int_1^\infty \partial\varphi/\partial x_j(tx)\, dt = \sum_1^n x_j \int_0^1 \partial\varphi/\partial x_j(tx)\, dt.$$

If $\varphi(x) = 0$ for $|x| \leqq 2$, let $\alpha \in C^\infty$ be 0 for $|x| \leqq 1$, and 1 for $|x| \geqq 2$, and take φ_j to be α times the integral in the first sum. If $\varphi(x) = 0$ for $|x| \geqq 3$, let $\alpha \in C_0^\infty$ be 1 for $|x| \leqq 3$, and take φ_j to be α times the integral in the second sum. Any φ in S is the sum of one that is 0 for $|x| \leqq 2$ and one that is 0 for $|x| \geqq 3$.

Note added in proof. Only recently, the authors were made aware of references [12]–[14], and some others, by E. I. Vainberg et al. The articles of Vainberg deal with parallel beam tomography; References [2], [9], and this article deal with both parallel and divergent (fan) beam tomography.

REFERENCES

[1] A. Faridani, *Praktische Fragen der lokalen Tomographie*, Z. Angew. Math. Mech., 70 (1990), pp. T530–T532.

[2] A. Faridani, F. Keinert, F. Natterer, E. L. Ritman, and K. T. Smith, *Local and global tomography*, Signal Process., IMA Vol. Math. Appl., Vol. 23, Springer-Verlag, New York, 1990, pp. 241–255.

[3] A. V. Lakshminarayanan, *Reconstruction from divergent x-ray data*, Suny Tech. Report 32, Comp. Sci. Dept., State University of New York, Buffalo, NY, 1975.

[4] G. N. Ramachandran and A. V. Lakshminarayanan, *Three dimensional reconstruction from radiographs and electron micrographs: application of convolutions instead of Fourier transforms*, Proc. Nat. Acad. Sci. U.S.A., 1971, pp. 2236–2240.

[5] L. A. Shepp and B. F. Logan, *The Fourier reconstruction of a head section*, IEEE Trans. Nuclear Sci., 1974, pp. 21–43.

[6] K. T. Smith, *A generalization of an inequality of Hardy and Littlewood*, Canad. J. Math., 1956, pp. 157–170.

[7] K. T. Smith, D. Solmon, and S. L. Wagner, *Practical and mathematical aspects of the problem of reconstructing objects from radiographs*, Bull. Amer. Math. Soc., 1977, pp. 1227–1270.

[8] K. T. Smith, *Reconstruction formulas in computed tomography*, Proc. Sympos. Appl. Math., No. 27, L. A. Shepp, ed., AMS, Providence, RI, 1983, pp. 7–23.

[9] K. T. Smith and F. Keinert, *Mathematical foundations of computed tomography*, Appl. Optics, 1985, pp. 3950–3957.

[10] S. L. Sobolev, *Sur un theoreme de l'analyse fonctionelle*, C. R. Acad. Sci. USSR, 1938, pp. 5–9.

[11] W. J. T. Spyra, A. Faridani, E. L. Ritman, and K. T. Smith, *Computed tomographic imaging of the beating heart—use of local tomography*, IEEE Trans. Med. Imag., (1990), pp. 1–4.

[12] E. I. Vainberg, I. A. Kazak, and V. P. Kurczaev, *Reconstruction of the internal three-dimensional structure of objects based on real-time integral projections*, Soviet J. Nondest. Test., 17 (1981), pp. 415–423.

[13] E. I. Vainberg, I. A. Kazak, and M. L. Faingoiz, *X-ray computerized back projection tomography with filtration by double differentiation. Procedure and information features*, Soviet J. Nondest. Test., 21 (1985), pp. 106–113.

[14] E. I. VAINBERG AND M. L. FAINGOIZ, *Increasing the spatial resolution in computerized tomography*, Problems in Tomographic Reconstruction, A. S. Alekseev, M. M. Lavrent'ev, and G. N. Preobrazhensky, eds., Siberian branch of Acad. Sci. USSR, Novosibirsk, (1985), pp. 28–35.

[15] D. O. WARNER, J. F. BRICHANT, E. L. RITMAN, AND K. REHDER, *Epidermal anaesthesia and intrathoracic blood volume*, British J. Anaesthesia, submitted.